JOURNAL OF AIRCRAFT
Vol. 45, No. 5, September–October 2008

# Tear Propagation of a High-Performance Airship Envelope Material

Shoji Maekawa*
*Japan and Japan Aerospace Exploration Agency (JAXA), Mitaka, Tokyo 181-0015, Japan*
Kouichi Shibasaki,† Toyotoshi Kurose,‡ Toshiyuki Maeda,† and Yoshitaka Sasaki‡
*Kawasaki Heavy Industries, Inc., Kakamigahara, Gifu 504-8710, Japan*
and
Tatsuya Yoshino§
*Taiyo Kogyo Corporation, Hirakata, Osaka 573-1132, Japan*

DOI: 10.2514/1.32264

**In a design criterion of a nonrigid airship, such as FAA-P-8110-2, Airship Design Criteria, it is specified to measure the tear strength of the envelope material. However, the tear strength itself has no definite relationship with the actual tear propagation characteristics of an airship envelope material. Therefore, there are several investigations to establish the relationship. To study it, tests are conducted to measure the tear propagation stress to find the appropriate formula. To simulate the actual stress field, two kinds of tests are carried out: a biaxial tensile test and a pressurized cylinder test. Both tests simulate the biaxial stress field on an airship envelope. The material tested is the high-strength and lightweight envelope material, Z2929T-AB. This is one of the envelope materials with Zylon as its base fabric and is developed especially for the technology demonstrator of a stratospheric platform. This material has a density as low as 157 g/m$^2$; nevertheless, the tensile strength is as high as 997 N/cm. The measurement is made to find the stress that initiates the tear propagation. The data are fitted to Thiele's formula and the correlation is excellent. By using Thiele's empirical equation, the minimum slit size of the tear propagation under the limit stress is estimated. For the technology demonstrator of the stratospheric platform, which is planned to have an overall length of 150 m and the maximum diameter of 38 m, the slit size of less than 40 mm does not allow tear propagation under the limit load. The consideration of the stress field near the slit introduces a different approach for the empirical formula, and this leads to the equation which correlates very well the tear propagation stress with the tensile strength of the envelope material. These two results are described, as well as the test details.**

## Nomenclature

| | | |
|---|---|---|
| $a$, $b$, $C_l$, $n$ | = | constants |
| $C_s$ | = | cut slit tear strength |
| $k$ | = | correction factor for cylinder curvature |
| $L$ | = | critical longitudinal slit length |
| $N$ | = | number of tests |
| $p$ | = | rupture pressure of the cylinder, internal pressure |
| $r$ | = | radius of the cylinder, radius of the envelope |
| $\rho_H$ | = | radius of curvature in the hoop direction |
| $\rho_L$ | = | radius of curvature in the longitudinal direction |
| $\sigma$ | = | envelope stress, force per unit width |
| $\sigma_H$ | = | hoop stress |
| $\sigma_L$ | = | longitudinal stress |
| $\sigma_{\text{ult}}$ | = | tensile strength |

Presented as Paper 7829 at the 7th AIAA Aviation Technology, Integration, and Operations Conference, and 2nd Centre of Excellence for Integrated Aircraft Technologies International Conference on Innovation and Integration in Aerospace Sciences, and 17th Lighter-Than-Air Systems Technology Conference, Hastings Europa Hotel, Belfast, Northern Ireland, 18–20 September 2007; received 21 May 2007; revision received 15 January 2008; accepted for publication 29 February 2008. 

*Professor, Department of Mechanical Engineering, 2200-2 Toyosawa; also Guest Researcher, Unmanned and Innovative Aircraft Team, 6-13-1 Osawa; currently Shizuoka Institute of Science and Technology, Fukuroi, Shizuoka 437-8555. Member AIAA.

†Assistant Manager, Engineering Division, Aerospace Company, 1 Kawasaki-cho.

‡Manager, Engineering Division, Aerospace Company, 1 Kawasaki-cho.

§Senior Research Engineer, Advanced Structures Research and Development Department, 3-20 Syodai-Tajika.

## I. Introduction

THE concept of a stratospheric platform, in which airships fly stationary in a stratosphere where the wind is relatively calm and act as a platform for communication, broadcasting, or earth observation, has been proposed [1] and several flight tests have been performed [2–4]. Because the air density at the altitude of 20 km is one-fourteenth of that on the ground, an airship whose buoyancy comes from the density difference between helium and air should increase its helium gas volume, so that it should be large sized. However, as the size gets larger, its ground operations including takeoff and landing become drastically more difficult. Therefore, it is desirable to make it as small as possible. Thus, it is most important to reduce the structural weight, and lightweight envelope materials are needed. The envelope materials with Zylon as the base fabric have been developed and their basic material properties have been obtained.

To ensure that the envelope material does not burst during its operation, it is necessary to obtain the tear propagation properties of the envelope materials. In a design criterion of a nonrigid airship, such as FAA-P-8110-2, Airship Design Criteria [5], it is specified to measure the tear strength of an envelope material. It also specifies that the tear would not propagate under the limit load condition. However, the tear strength itself has no definite relationship with the actual tear propagation characteristics of the airship envelope material. Therefore, there have been several studies to establish the relationship. They are reviewed briefly.

Two kinds of tear propagation tests are conducted to obtain the tear propagation properties of the lightweight Zylon envelope material. A cruciform specimen biaxial tensile test is conducted for a short slit, and the tear propagation stress is measured as well as the burst stress. A pressurized cylinder test is also conducted for a rather long slit and the tear propagation stress is measured. The results are examined for compatibility with Thiele's formula. Another approach, based on the stress field consideration near the slit, is also tried to obtain the

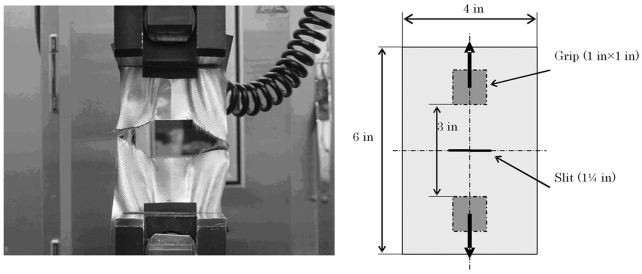


**Fig. 1 Cut slit tear strength test [5].**

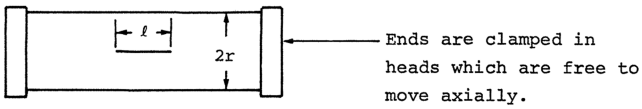


**Fig. 2 Slit cylinder test [6].**

empirical equation of the tear propagation. Finally, the allowable slit length for the technology demonstrator of the stratospheric platform is estimated.

Note that the term stress is defined in this paper as a force per unit width, which is a common practice in airship envelope studies.

## II. Past Research on Tear Propagation

For the tear propagation of airship envelope materials, FAA-P-8110-2, Airship Design Criteria, specifies the tear test (Fig. 1) to obtain the cut slit tear strength $C_s$ and requires that the tear should not propagate under its limit load condition. However, $C_s$ is not the tear propagation stress itself, and so research to correlate it with the tear propagation stress has been conducted.

Topping [6] measured the rupture stresses of a pressurized cylinder with a cut slit made of Dacron-neoprene envelope material (Fig. 2). The measured data are summarized in Table 1. Several theories were applied to correlate with the measured data, but it was concluded that no theory satisfies the validity. However, the modified Griffith theory coincides well with the measured data, as shown in Fig. 3.

$$\sigma = pr = \frac{C_l}{L^n[1 + k(L/r)]} \tag{1}$$

where $p$ is the rupture pressure of the cylinder, $r$ is the radius of the cylinder, $C_l$ and $n$ are the constants, $L$ is the slit length, and $k$ is the correction factor for cylinder curvature. The drawback of this formula is that the least-square method cannot be used because of the empirical constant $k$. Instead, Topping has substituted three data points into Eq. (1) to obtain the empirical constants.

Lagerquist and Keen [7] performed the burst test of Kevlar envelope material as shown in Fig. 4, and showed the relationship between initial slit length and critical tear stress in Fig. 5.

Here, let us recall the fundamental equations of the stress field on the envelope of a nonrigid airship [8]. The longitudinal and hoop stresses of a body of rotation with the radius $r(x)$ under internal pressure $p$ can be expressed as a function of the radii of curvature in the hoop direction $\rho_H$ and in the longitudinal direction $\rho_L$;

$$\sigma_L(x) = \frac{1}{2} p\rho_H(x) \tag{2}$$

$$\sigma_H = p\rho_H(x)\left(1 - \frac{1}{2}\frac{\rho_H}{\rho_L}\right) \tag{3}$$

$$\rho_H(x) = r(x)\{1 + [r'(x)]^2\}^{\frac{1}{2}} \tag{4}$$

$$\rho_L(x) = \left|\frac{\{1 + [r'(x)]^2\}^{\frac{2}{3}}}{r''(x)}\right| \tag{5}$$

Here, $r'(x) = \mathrm{d}r(x)/\mathrm{d}x$.

The bending moment caused by flight loads is the maximum at the midsection of the envelope. The envelope can be approximated to a cylinder in the vicinity of the midsection. In this case,

$$\rho_H = r(x) \tag{6}$$

$$\rho_L = \infty \tag{7}$$

$$\sigma_L(x) = \frac{1}{2} pr(x) \tag{8}$$

**Table 1 Slit cylinder burst data for fabric N337A15 (single-ply Dacron-neoprene) [6]**

| Slit length $l$, mm (in.) | Slit width,[a] mm (in.) | Cylinder | | Burst pressure $p$, kPa (psi) | $l/r$ | $pr$, N/cm (lb/in.) |
|---|---|---|---|---|---|---|
| | | Diameter $2r$, mm (in.) | Length, mm (in.) | | | |
| 25.4 (1.0) | $25.4/c_x$ $(1/c_x)$ | 203 (8.0) | 460 (18) | 57 (8.3) | 0.25 | 58.1 (33.2) |
| | | | 610 (24) | 62 (9) | | 63.0 (36.0) |
| | | | | 58 (8.4) | | 63.0 (33.6) |
| | | | | 57 (8.3) | | 58.1 (33.2) |
| | | | 760 (30) | 60 (8.7) | | 60.9 (34.8) |
| | | | 910 (36) | 59 (8.5) | | 59.5 (34.0) |
| | $50.8/c_x$ $(2/c_x)$ | | 610 (24) | 58 (8.4) | | 58.8 (33.6) |
| | $76.2/c_x$ $(3/c_x)$ | | | 58 (8.4) | | 58.8 (33.6) |
| | $102/c_x$ $(4/c_x)$ | | | 61 (8.9) | | 62.3 (35.6) |
| 38.1 (1.5) | $25.4/c_x$ $(1/c_x)$ | | | 44 (6.4) | 0.375 | 44.8 (25.6) |
| 57.2 (2.25) | | | | 27 (3.9) | 0.562 | 27.3 (15.6) |
| 85.7 (3.375) | | | | 21 (3.0) | 0.843 | 21.0 (12.0) |
| 17.5 (0.69) | $25.4/c_x$ $(1/c_x)$ | 135.4 (5.33) | 460 (18) | 113 (16.4) | 0.25 | 76.7 (43.8) |
| 25.4 (1.0) | | | | 81 (11.8) | 0.375 | 55.2 (31.5) |
| 38.1 (1.5) | | | | 57 (8.2) | 0.562 | 38.4 (21.9) |
| 57.2 (2.25) | | | | 37 (5.4) | 0.843 | 25.2 (14.4) |
| 25.4 (1.0) | $25.4/c_x$ $(1/c_x)$ | 305 (12.0) | 910 (36) | 41 (5.9) | 0.167 | 62.0 (35.4) |
| 38.1 (1.5) | | | | 31 (4.5) | 0.25 | 47.3 (27.0) |
| 57.2 (2.25) | | | | 21 (3.0) | 0.375 | 31.5 (18.0) |
| 85.7 (3.375) | | | | 15.2 (2.2) | 0.562 | 21.1 (13.2) |
| 128.6 (5.0625) | | | | 9.7 (1.4) | 0.843 | 14.7 (8.4) |

[a]Number of fill threads per inch $= c_x$.

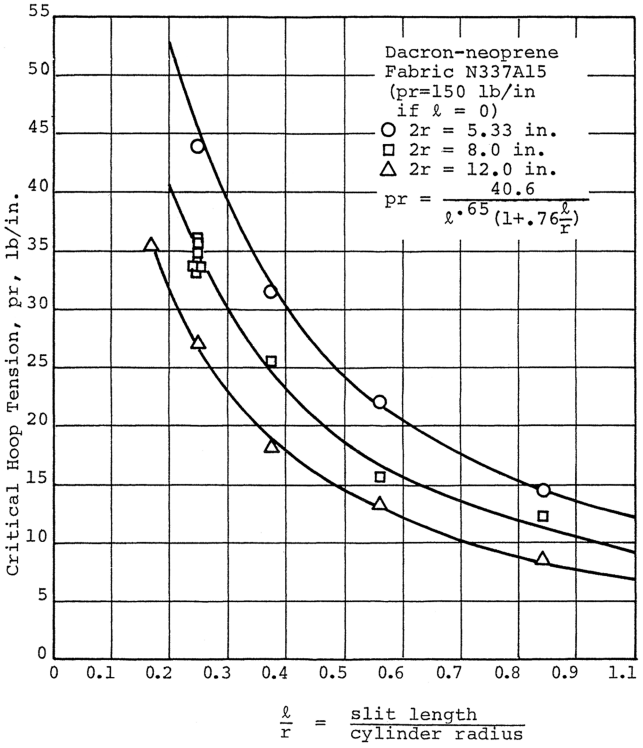


**Fig. 3 Modified Griffith theory with the measured data [6].**

$$\sigma_H(x) = pr(x) \tag{9}$$

As shown in Eqs. (8) and (9), the longitudinal stress due to the internal pressure is half of the hoop stress, and the stress is proportional to the radius of the envelope. The stress caused by the internal pressure also gets its maximum value at the midsection of the envelope where the radius is the maximum. It is preferable to conduct the tear propagation test with a cylindrical specimen to simulate this biaxial stress field.

Miller and Mandel [9] carried out the tear propagation test with ILC cylinders (ILC Dover), as shown in Fig. 6, and confirmed that Thiele's empirical formula, which correlates cut slit tear strength $C_s$ with tear propagation stress, can be applied to the envelope material of Zeppelin NT (Fig. 7).

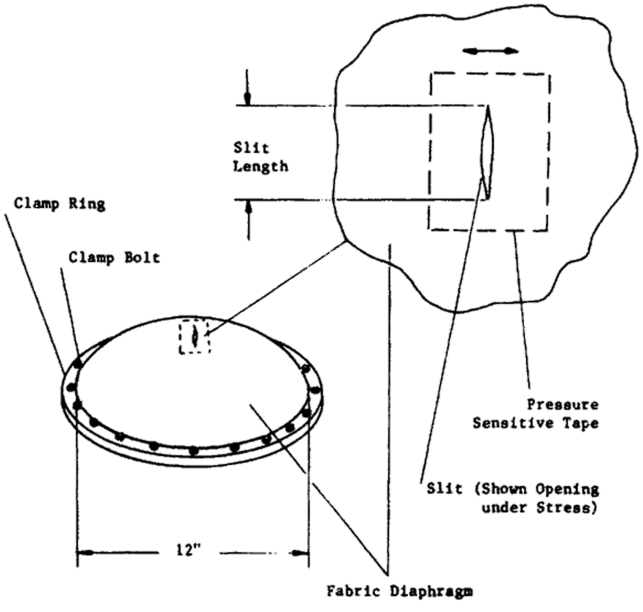


**Fig. 4 Burst test of Kevlar envelope material [7].**

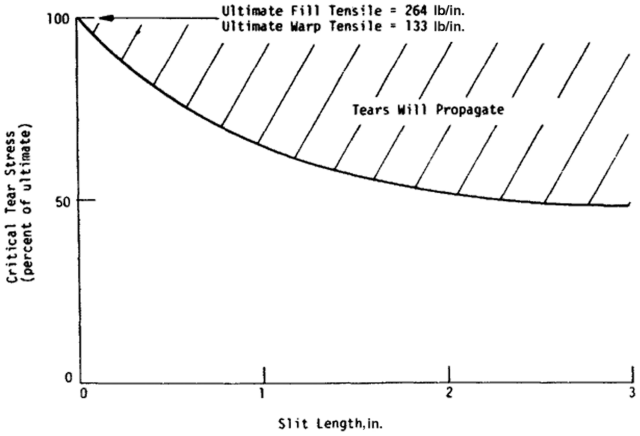


**Fig. 5 Tear propagation property of Kevlar envelope material [7].**

$$\sigma = pr = \frac{1.4C_s}{L^{0.525}(1 + L/r)} \tag{10}$$

where $L$ is the critical longitudinal slit length.

## III. Zylon Envelope Material

To reduce the structural weight, high-strength and lightweight envelope materials have been developed. In the early phase of the development, high strength is the top priority and Z4040T-AB has been developed. The base fabric of Z4040T-AB is Zylon (PBO, Toyobo) and the density is 203 $g/m^2$. The tensile strength in the weft direction is 1310 N/cm. This material suits the operational airship, which is planned to have an overall length of 250 m. However, it has too much strength for the 150 m class technology demonstrator planned in the process of the stratospheric platform development [10]. Therefore, the lighter-weight envelope material, Z2929T-AB, has been developed [11,12]. This material also uses Zylon as its base fabric. The tensile strength in the warp direction is 997 N/cm and the density is 157 $g/m^2$. The layer composition of Z2929T-AB is shown in Fig. 8. The layer composition of Z4040T-AB is the same. The typical material properties are shown in Figs. 9 and 10. In the xenon test, the specimens are exposed to 180 $W/m^2$ xenon light for 100 h, which is equivalent to half of a year's exposure to ultraviolet rays on the ground. Ozone at $50 \pm 5$ ppm is applied to the specimens for 24 h

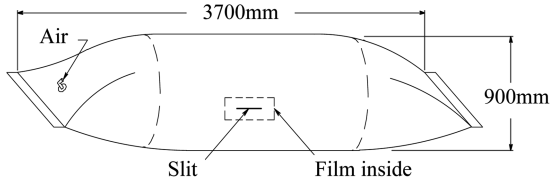


**Fig. 6 ILC cylinder [9].**

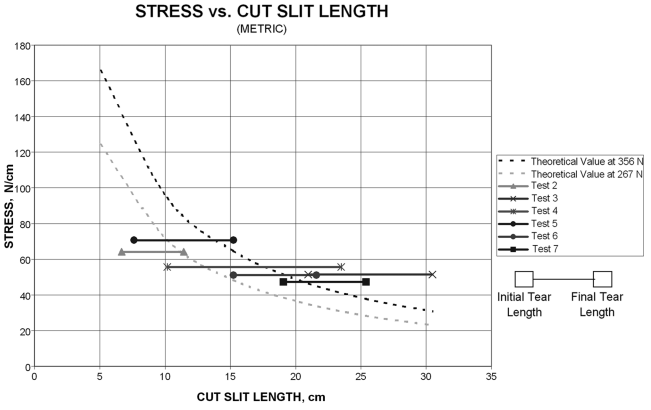


**Fig. 7 Compatibility of Thiele's formula with test data [9].**

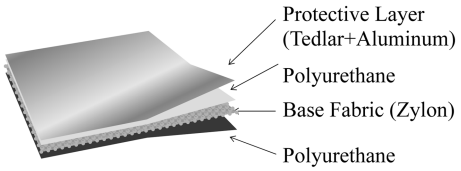


**Fig. 8 Layer composition of Z2929T-AB.**

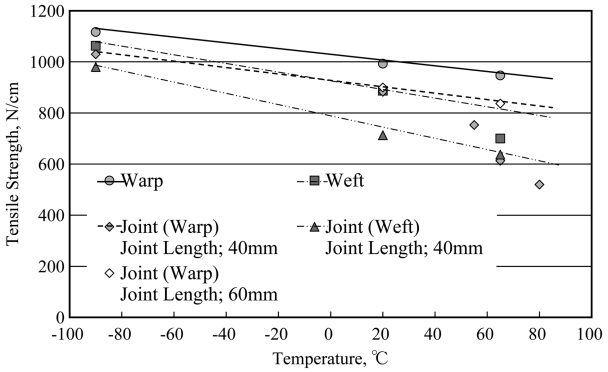


**Fig. 9 Tensile strength of Z2929T-AB.**

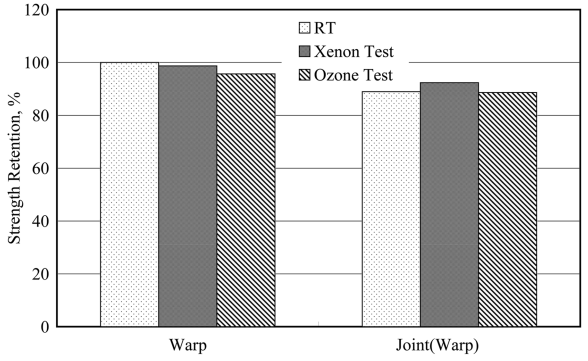


**Fig. 10 Residual strength of Z2929T-AB after accelerated environmental exposure [11].**

in the ozone test. This ozone density is five times higher than that at the altitude of 20 km.

## IV. Test Method

To obtain the tear propagation characteristics, two kinds of test methods are applied: a cruciform specimen biaxial tensile test and a pressurized cylinder test [13] similar to ILC cylinder test.

### A. Cruciform Specimen Biaxial Tensile Test

The specimen of the cruciform specimen biaxial test is shown in Fig. 11. The slit which simulates the tear in the hull is applied along the weft direction at the center of the specimen by a razor. The length of the slit is 10, 20, or 50 mm. Three specimens are tested for each slit length.

The specimens are set in the test apparatus shown in Fig. 12. The tensile load is increased at the speed of 1 mm/ min in the warp direction. The tensile load in the weft direction simulates the actual stress field, so that the speed is controlled to 50% of the warp direction. Thus, the biaxial tensile load is applied in strain control mode with a strain ratio of 1:2. The status of the slit is recorded by a video camera, and the time when the tear starts to propagate is identified from the video record. The tensile load at which the tear starts to propagate is then obtained from the tensile load record in the warp direction at the identified time. The load is divided by the width of the specimen, 400 mm, to obtain the stress.

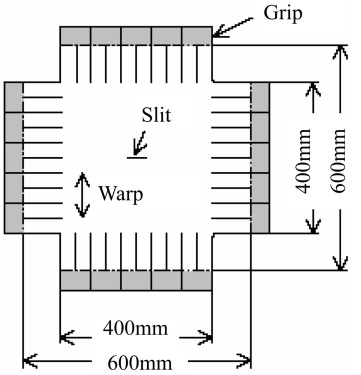


**Fig. 11 Test specimen of cruciform specimen biaxial tensile test.**

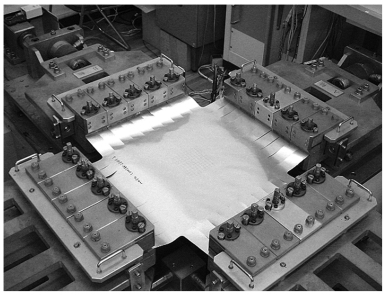

**Fig. 12 Test setup of cruciform specimen biaxial tensile test.**

### B. Pressurized Cylinder Test

Using the air pressurized cylinder to generate the biaxial tensile field is a popular method in the development of airships. This method simulates the actual stress field, and longer tear length can be tested compared to the cruciform specimen biaxial tensile test. In this test, the biaxial load is applied in stress control mode. When the slit is parallel to the longitudinal direction of the cylinder, the tear propagates at a lower stress than a flat specimen due to the so-called bulge effect. Therefore, the measured results should be corrected to account for this effect.

The specimen is a cylinder closed at both ends and the size is 4.0 m in length and 0.9 m in diameter, as shown in Fig. 13. The slit is covered from inside by an expandable film to prevent air leakage. The initial slit length is 70 mm and two specimens are prepared.

The test setup is shown in Fig. 14. The specimen is set in the test stand and the pressure is increased at the speed of 1 kPa/ min. The slit is watched and recorded by a video camera. The pressurization is stopped immediately when the tear starts to propagate and depressurization is made. The time when the tear starts to propagate is identified from the video record after the test. The pressure value is identified from the pressure record at the identified time. The stress is then calculated by multiplying the radius of the cylinder, 0.45 m, to the pressure value.

After depressurization, the slit is expanded to set a new initial slit length. The test is conducted for eight cases of the initial tear length from 70 to 200 mm for two specimens.

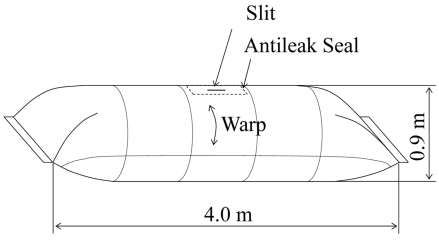


**Fig. 13 Pressurized cylinder test specimen.**

## V. Test Result and Empirical Formulation

The test results obtained by both methods are shown in Fig. 15 and Tables 2 and 3. The cut slit tear strength is obtained as an average of five specimens; $C_s = 350$ N. To obtain the empirical formula for the tear propagation characteristics of the envelope material, two approaches are tried. The first approach is Thiele's formula, which is proposed for the envelope material and used for the envelope material of Zeppelin NT. The other one is based on the consideration of the stress field near the slit tip.

### A. Thiele's Empirical Formula

The general expression of Thiele's empirical formula can be written as follows [9]:

$$\sigma = pr = \frac{C_l C_s}{L^n(1 + L/r)} \tag{11}$$

For the flat specimen, this equation becomes

$$\sigma = \frac{C_l C_s}{L^n} \tag{12}$$

In the preceding equations, $C_l$ and $n$ are the constants. To decide these constants, the least-square method is applied. Because the constant $n$ is in the denominator of the equation, logarithms of both sides of Eq. (11) are taken and then the least-square method is applied. Then, the constants $C_l$ and $n$ are obtained from the following equations:

$$C_l = \exp\left[\frac{D(B + C) - A(F + G) - E(ND - A^2)}{ND - A^2}\right] \tag{13}$$

$$n = \frac{A(B + C) - N(F + G)}{ND - A^2} \tag{14}$$

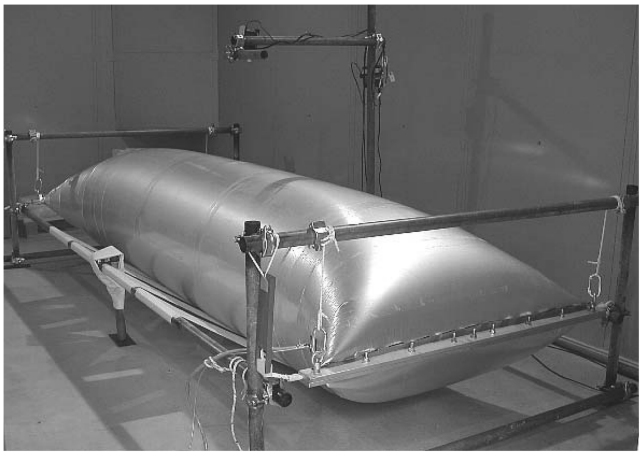

**Fig. 14 Test setup of pressurized cylinder test.**

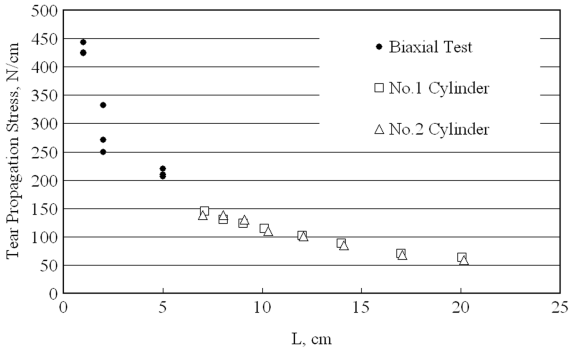


**Fig. 15 Test result of Z2929T-AB.**

where

$$A = \sum_{i=1}^{N} \ell_n L_i \tag{15}$$

$$B = \sum_{i=1}^{N} \ell_n \sigma_i \tag{16}$$

$$C = \sum_{i=1}^{N} \ell_n\left(1 + \frac{L_i}{r_i}\right) \tag{17}$$

$$D = \sum_{i=1}^{N} \ln^2 L_i \tag{18}$$

$$E = \ell_n C_s \tag{19}$$

$$F = \sum_{i=1}^{N} \ell_n L_i \, \ell_n\left(1 + \frac{L_i}{r_i}\right) \tag{20}$$

$$G = \sum_{i=1}^{N} \ell_n L_i \, \ell_n \sigma_i \tag{21}$$

Substituting the test results, including the biaxial test results with $r_i = \infty$, into these equations, the constants were obtained:

$$C_l = 1.238 \qquad n = 0.503$$

Therefore, Thiele's formula for Z2929T-AB is expressed as

$$\sigma = \frac{1.238 \times 350}{L^{0.503}[1 + (L/r)]} \tag{22}$$

Here, the unit system is $\sigma$ N/cm, $C_s$ N, $L$ cm, and $r$ cm.

In Fig. 16, the test data are plotted with the empirical formula. The biaxial tensile test uses a flat specimen, so that the value in parentheses in the denominator is set to one to draw the empirical line for a flat panel. They agree quite well. Therefore, it can be concluded that Thiele's empirical formula can be applied to the Zylon envelope material.

### B. Stress Field Consideration

To investigate the relationship between the tear propagation stress and the tensile strength of the material, another empirical formula is studied. As shown in Fig. 17, the stress is assumed to distribute exponentially near the slit tip. Therefore,

$$\sigma(x) = \sigma_\infty + ae^{-bx} \tag{23}$$

Here, $\sigma_\infty$ is the uniform stress at the infinitely distant field, $a$ and $b$ are the constants to simulate the stress concentration near the slit tip. The load within the slit region is distributed as a stress concentration outside the slit region.

$$\int ae^{-bx}\,dx = \frac{1}{2}L\sigma_\infty \tag{24}$$

Therefore,

**Table 2 Biaxial tensile test result**

| Initial slit length, mm | No. | Stress to start tear propagation, N/cm | Slit length at the maximum stress, mm | Maximum stress, N/cm |
|---|---|---|---|---|
| 10 | 1 | 443 | 11.2 | 443 |
| | 2 | 425 | 12.3 | 425 |
| | 3 | 424 | 11.4 | 424 |
| | Average | 431 | 11.6 | 431 |
| 20 | 1 | 271 | 23.0 | 326 |
| | 2 | 250 | 22.7 | 323 |
| | 3 | 332 | 26.4 | 340 |
| | Average | 284 | 24.0 | 330 |
| 50 | 1 | 220 | 82.6 | 256 |
| | 2 | 206 | 82.6 | 248 |
| | 3 | 210 | 60.5 | 261 |
| | Average | 212 | 75.3 | 255 |

**Table 3 Pressurized cylinder test result**

| Specimen no. | Diameter, mm | Temperature, °C | Initial slit length, mm | Pressure to start tear propagation, kPa | Stress to start tear propagation, N/cm |
|---|---|---|---|---|---|
| No. 1 | 899 | 8.0 | 50.5 | [a] | —— |
| | | 8.0 | 61.0 | [a] | —— |
| | | 4.8 | 71.0 | 32.2 | 145 |
| | | 7.1 | 80.5 | 29.0 | 130 |
| | | 3.6 | 90.5 | 27.5 | 124 |
| | | 3.8 | 101.0 | 25.3 | 114 |
| | | 4.0 | 120.2 | 22.6 | 102 |
| | | 3.9 | 140.0 | 19.8 | 89 |
| | | 4.2 | 170.0 | 15.6 | 70 |
| | | 4.1 | 200.7 | 14.0 | 63 |
| No. 2 | 899 | 4.8 | 70.0 | 30.7 | 138 |
| | | 4.7 | 80.5 | 30.6 | 138 |
| | | 4.7 | 91.0 | 28.9 | 130 |
| | | 4.9 | 103.0 | 24.5 | 110 |
| | | 4.5 | 120.7 | 22.5 | 101 |
| | | 4.5 | 141.0 | 18.8 | 85 |
| | | 5.0 | 170.6 | 15.2 | 68 |
| | | 5.1 | 201.5 | 13.2 | 59 |

[a]No propagation (~33.5 kPa)

$$\frac{a}{b} = \frac{1}{2} L\sigma_\infty \tag{25}$$

If it is assumed that the tear starts to propagate when the fiber stress at the slit tip reaches the ultimate strength of the envelope material $\sigma_{ult}$, the following relation can be introduced from Eq. (23):

$$\sigma_\infty + a = \sigma_{ult} \tag{26}$$

From Eqs. (25) and (26), the following equation is obtained:

$$\sigma_\infty = \frac{2\sigma_{ult}}{2 + bL} \tag{27}$$

This equation can be the empirical expression of the tear propagation stress if the value of the constant $b$ is found from the test data. Now, the uniform stress, far apart from the slit tip, $\sigma_\infty$ is replaced by $\sigma$ in the same way of expression as the foregoing section:

$$\sigma = \frac{2\sigma_{ult}}{2 + bL} \tag{28}$$

In the process of introducing the preceding equation, the bulge effect is not considered. The so-called bulge effect is induced because of the curvature. When a slit is on a cylinder in the direction of the longitudinal axis, the envelope tends to protrude in the vicinity of the slit because the circumferential constraint no longer exists. This effect induces the out-of-plane tearing stress on the material and changes the tear propagation characteristics. Topping [6] introduces this effect by dividing the stress by $1 + k(L/r)$. Here, $k$ is another empirical constant. Thiele uses the simpler term $1 + L/r$. In this study, Thiele's correction follows. To include the bulge effect, the preceding equation is modified to

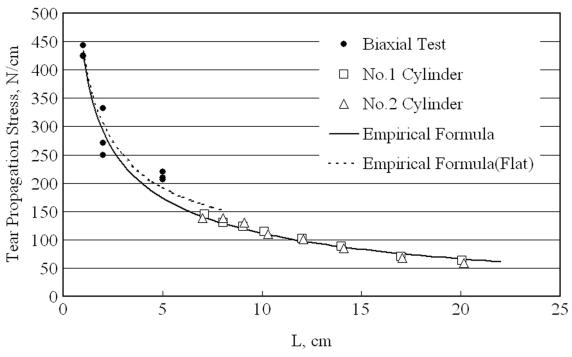


**Fig. 16 Thiele's formula with Z2929T-AB test result.**

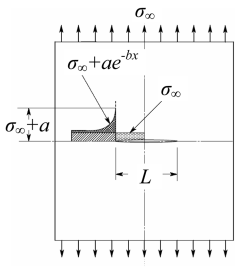


**Fig. 17 Stress field in the vicinity of the slit.**

$$\sigma = \frac{2\sigma_{\text{ult}}}{(2 + bL)[1 + (L/r)]} \tag{29}$$

To obtain the constant $b$, the least-square method is again applied to the logarithms of both sides of the equations. However, no explicit solutions are obtained. Instead, the following equations should be solved for a finite value of $b$ through a trial and error process. For the empirical formula without the bulge effect,

$$\sum_{i=1}^{N} \frac{L_i[\ell_n(2 + bL_i) + \ell_n \sigma_i - \ell_n 2\sigma_{\text{ult}}]}{2 + bL_i} = 0 \tag{30}$$

For the empirical formula with the bulge effect,

$$\sum_{i=1}^{N} \frac{L_i\{\ell_n(2 + bL_i) + \ell_n \sigma_i - \ell_n 2\sigma_{\text{ult}} + \ell_n[1 + (L_i/r_i)]\}}{2 + bL_i} = 0 \tag{31}$$

By applying the test data into these equations, the constant $b$ is obtained. For the case without the bulge effect,

$$b = 1.441$$

$$\sigma = \frac{2 \times 900}{2 + 1.441L} \tag{32}$$

For the case with the bulge effect,

$$b = 1.153$$

$$\sigma = \frac{2 \times 900}{(2 + 1.153L)[1 + (L/r)]} \tag{33}$$

Here, the unit system is $\sigma$ N/cm, $L$ cm, and $r$ cm. Note that 900 N/cm is used here as the tensile strength of Z2929T-AB, instead of 997 N/cm. This value is obtained for the material lot tested in this report. The discrepancy may be induced due to inappropriateness of the manufacturing process. The cause is under investigation.

Figure 18 shows the comparison between the test results and the empirical formula without the bulge effect. They agree very well. Figure 19 shows the comparison when the bulge effect is considered. The agreement is also good.

To study the applicability of this approach, the preceding equations are applied to Topping's data [6] shown in Table 1, which contains three sizes of the cylinder radius. For the case without the bulge effect,

$$b = 2.70$$

$$\sigma = \frac{2 \times 263}{2 + 2.70L} \tag{34}$$

For the case with the bulge effect,

$$b = 1.77$$

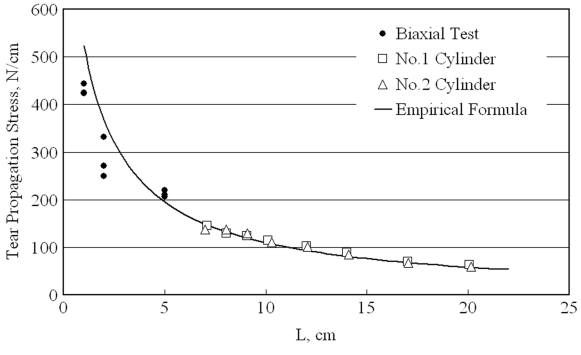


**Fig. 18 Empirical formula without the bulge effect.**

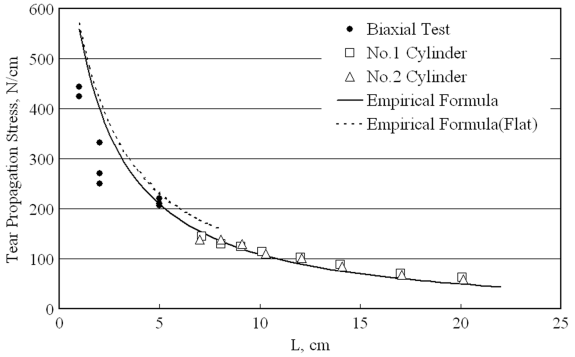


**Fig. 19 Empirical formula with the bulge effect.**

$$\sigma = \frac{2 \times 263}{(2 + 1.77L)[1 + (L/r)]} \tag{35}$$

Here, the unit system is $\sigma$ N/cm, $L$ cm, and $r$ cm.

Figure 20 shows the comparison between the test results and the empirical formula, Eq. (34), without the bulge effect consideration. Figures 21 and 22 show the comparison with Eq. (35) when the bulge effect is considered. Although the bulge effect is seen in the test results, it is not prominent. The empirical formula also shows the difference for each radius when the bulge effect is considered. However, the compatibility with the test results is better when the bulge effect is not included.

Here, the empirical formula based on the stress concentration at the slit tip is applied to both the Zylon envelope material and Topping's data [6]. In both cases, the empirical formula without the bulge effect simulates the test data better than that with the bulge effect.

## VI. Allowable Slit Size

It is specified in FAA-P-8110-2, Airship Design Criteria [5], that the tear would not propagate under the limit load condition. The planned technology demonstrator of the stratospheric platform has a length of 150 m and a maximum diameter of 38 m. The tear

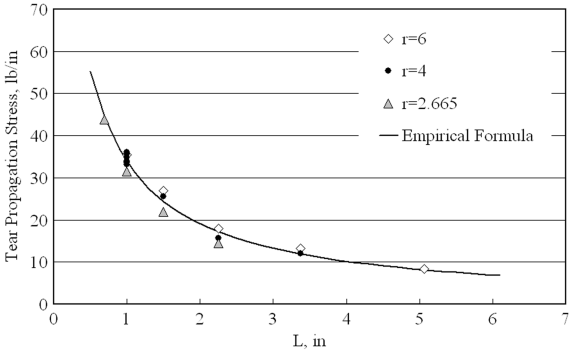


**Fig. 20 Empirical formula for Topping's data without the bulge effect [6].**

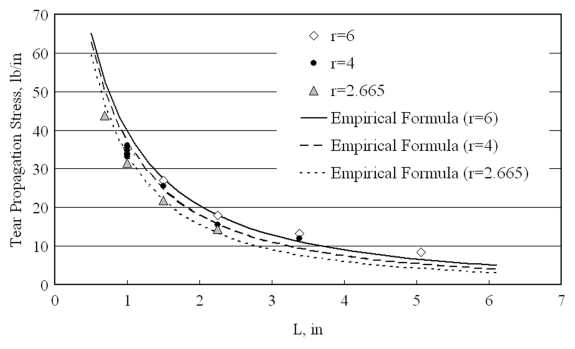


**Fig. 21 Empirical formula for Topping's data with the bulge effect [6].**

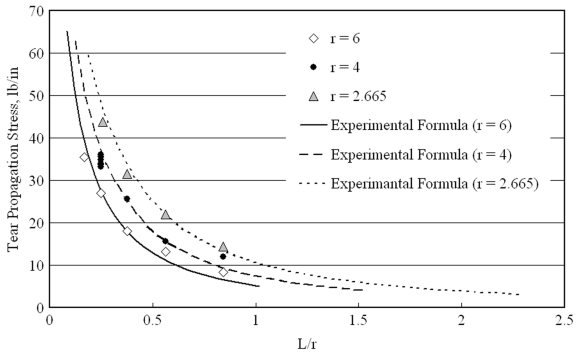


**Fig. 22 Empirical formula for Topping's data with the bulge effect [6].**

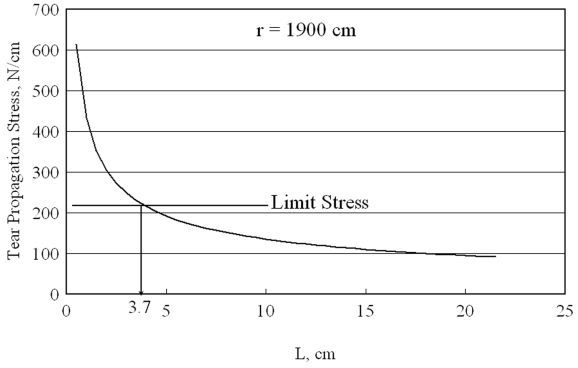


**Fig. 23 Allowable slit size of the technology demonstrator.**

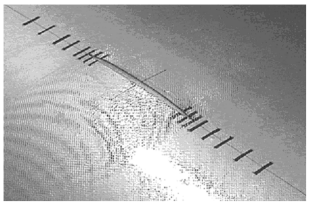

**Fig. 24 Peripheral appearance of the slit.**

propagation characteristics of the Zylon envelope material Z2929T-AB at the maximum diameter can be expressed as

$$\sigma = \frac{1.238 \times 350}{L^{0.503}[1 + (L/1900)]} \tag{36}$$

or

$$\sigma = \frac{2 \times 900}{2 + 1.441L} \tag{37}$$

The former equation is Thiele's expression and the latter is the empirical formula proposed in this paper. The latter equation is the same as Eq. (32) because it is not a function of the radius.

If the limit stress of the envelope material is assumed to be 225 N/cm, the minimum slit size above which the tear propagates is estimated to be 37 mm, from Fig. 23, which is the graphical presentation of Eq. (36). If Eq. (37) is used, the minimum slit size is 42 mm. Therefore, the technology demonstrator can withstand up to about 40 mm slits.

As shown in Fig. 24, the fiber direction becomes oblique due to the shear stress caused by the stress concentration in the vicinity of the slit, and the surface condition differs clearly from the other area. Moreover, due to the lack of circumferential restraint, the envelope protrudes at the slit. Because of this, a slit in the Zylon envelope material is very detectable, and so a slit of much smaller size than 40 mm can be detected easily.

## VII. Conclusions

The tear propagation characteristics of the lightweight and high-strength Zylon envelope material are obtained experimentally. Empirical formulas for the tear propagation are examined and Thiele's formula is found applicable to the Zylon envelope material. The consideration of the stress field in the vicinity of the slit tip leads to another formula, and this formula is also found to fit to the Zylon envelope material. The allowable slit size above which the tear propagates under the limit load condition is estimated using the preceding empirical formulas and is found to be about 40 mm. The slit in the Zylon envelope material is easily detectable and this value would not be critical.

## References

[1] Shimizu, T., "Japanese SPF Airship Project Progress," *Fifth Stratospheric Platform Systems Workshop*, SPSW2005 Organizing Com., Tokyo, Feb. 2005, pp. 15–22.

[2] Sasa, S., Yoshida, H., Ohashi, K., and Miyazaki, T., "Flight Test Overview of Ground to Stratosphere Flight Test Vehicle," *Fifth Stratospheric Platform Systems Workshop*, SPSW2005 Organizing Com., Tokyo, Feb. 2005, pp. 123–128.

[3] Nakadate, M., "Development and Flight Test of SPF-2 Low Altitude Stationary Flight Test Vehicle," *AIAA 5th Aviation, Integration, and Operations Conference*, AIAA 2005-7408, Sept. 2005.

[4] Maekawa, S., and Takegaki, A., "On the Structures of the Low Altitude Stationary Flight Test Vehicle," *AIAA 5th Aviation, Integration, and Operations Conference*, AIAA2005-7407, Sept. 2005.

[5] Federal Aviation Administration, "Airship Design Criteria," FAA-P-8110-2 CHG 2, 1995.

[6] Topping, A. D., "Critical Slit Length of Pressurized Coated Fabric Cylinders," Goodyear Aerospace Corp. GER-15879, 1973.

[7] Lagerquist, D. R., and Keen, L. B., "Structural Design of a High-Altitude Superpressure Powered Aerostat," *AIAA Lighter-Than-Air Technology Conference*, AIAA 1975-933, July 1975.

[8] Kraska, M., "Structural Analysis of the CL160 Airship," *14th Lighter-Than-Air Technical Committee Convention and Exhibition*, AIAA Paper, 2001.

[9] Miller, T., and Mandel, M., "Airship Envelopes: Requirements, Materials and Test Methods," *3rd International Airship Convention and Exhibition 2000*, AIAA Paper 2000-A19, 2000.

[10] Sasaki, S., Eguchi, K., Kouno, T., and Maekawa, S., "Scenario for Development of the SPF Airship Technology Demonstrator," *Fifth Stratospheric Platform Systems Workshop*, SPSW2005 Organizing Com., Tokyo, 2005, pp. 191–198.

[11] Maekawa, S., Maeda, T., Sasaki, Y., and Kitada, T., "Development of Advanced Lightweight Envelope Materials for Stratospheric Platform Airship," *43rd Aircraft Symposium, Aeronautical and Space Sciences Japan*, Japan Society for Aeronautical and Space Sciences Paper 2005-1B12, Oct. 2005, pp. 120–124.

[12] Maekawa, S., Hiyoshi, M., Sasaki, Y., and Segawa, S., "Evaluation of Reinforcement Methods Around a Circular Opening in High-Strength and Light-Weight Envelope Materials," *43rd Aircraft Symposium, Aeronautical and Space Sciences Japan*, Japan Society for Aeronautical and Space Sciences Paper 2005-1B11, Oct. 2005, pp. 113–119.

[13] Maekawa, S., Shibasaki, K., Maeda, T., Sasaki, Y., and Yoshino, T., "Crack Propagation Characteristics of Envelope Materials for a Stratospheric Platform Airship," *44th Aircraft Symposium, Aeronautical and Space Sciences Japan*, Japan Society for Aeronautical and Space Sciences Paper 2006-1D2, Oct. 2006, pp. 214–217.